Int. J. Electrochem. Sci., 12 **(2017)** 6340 – 6351, doi: 10.20964/2017.07.34

International Journal of
ELECTROCHEMICAL
SCIENCE
www.electrochemsci.org

TiN Supported Cobalt and Molybdenum Nitrides as an Efficient Oxygen Reduction Reaction Catalyst in Acid Medium

Qiuchan Huang, Shengzhou Chen[*]*,Tingting Ma, Hanbo Zou, Wei Yang*

School of Chemistry and Chemical Engineering, Guangzhou University, Guangzhou, China
[*]E-mail: szchen@gzhu.edu.cn

Received: 3 April 2017 / *Accepted:* 3 May 2017 / *Published:* 12 June 2017

TiN supported Co-Mo nitride nano particles were synthesized via a modified sol-gel method, and then nitrided under NH_3 atmosphere at 700 ℃. The samples obtained were characterized by XRD, XPS, HRTEM and SAED techniques and tested as catalysts for oxygen reduction reactions (ORR) in acid medium. The synergistic effect of the cobalt and molybdenum nitrides on nanosized TiN leads to a good ORR catalytic activity. The onset potential for the Co_1Mo_1Nx/TiN-6 catalyst was shifted to a more positive value 0.347 V versus SCE and the reduction peak located at 0.273 V versus SCE (0.401 V of Pt/C at the same condition). The number of electron transfer was tested by a rotating disk electrode which was in concordance with a two-electron mechanism at the potential 0.2 V versus SCE and it increased to four-electron in the negative values of the potential -0.2 V versus SCE. HRTEM showed that the nanoscale Co_2N and MoN were still highly dispersed on the surface of TiN though heated at high temperature. This work clearly indicates that the oxygen reduction active center of Co-Mo-N/TiN catalyst was the mixture of Co_2N and MoN.

Keywords: Modified sol-gel method, non-noble metal catalyst, ORR, TiN

1. INTRODUCTION

Proton exchange membrane fuel cells(PEMFCs) as clean and efficient energy converting devices have attracted enormous attentions recently. And Pt nano particle catalysts, supported on high-surface-area carbonaceous materials, represent state-of-the-art electrocatalysts for oxygen reduction reaction(ORR) at the PEMFCs anode and cathode, respectively [1-3]. However, the prohibitive price, scarcity of platinum and low durability of carbon supports have limited their widespread implementation in PEMFCs, especially for the ORR at the cathode that accounts for approximately 80% Pt loading ratio in fuel cell electrodes [4]. Therefore, searching for new catalysts with high activity, durability and low cost for cathode oxygen reduction reaction is vital. Recent studies have

showed that Pt-Co alloy deposition on carbon support exhibited excellent ORR activity, which is with a less noble metal using [5,6]. To date, carbon supported non-noble metal nitride (M-N-C) materials are generally considered as a promising ORR catalyst since the interaction between transition metals and C-N bonds can make a positive effect on oxygen reduction performance [7-10]. The transition metal on M-N-C catalysts often plays an important role in the direct participation in the active site and in situ formation of various carbon containing nitrogen nanostructures by catalyzing the decomposition of the nitrogen/carbon precursor [11]. The most active M-N-C catalysts reported were prepared using a metal salt, phenanthroline or NH_3 gas or cyanamide, and a microporous carbon black as Fe-, N- and C-precursors, respectively [12]. However, the durability of carbon based catalyst is relatively low in acid medium.

Titanium nitride (TiN) belongs to the three bonds transition metal compound, which has excellent chemistry inertia, high mechanical hardness and melting point [13-15]. And the electrical conductivity of TiN is 4000 s/cm, while presenting 1190 s/cm in carbon support [16]. Also, the electrochemical oxidation resistance of TiN is significantly better than that of carbon black [17, 18]. Because the oxide or oxynitride layers are formed on the TiN surface while the catalyst is scanned repeatedly by electrochemical workstation, which protect and strengthen the catalyst.

Pt/TiN as the oxygen reduction catalyst in PEMFCs has been reported recently. Several research have revealed that the activation or passivation of TiN nano particle supports have no effect on the electrochemical stability of Pt/TiN, upon subjecting to accelerated durability test [19, 20]. However, few reports of TiN supported non-noble metal electrocatalysts are available. Through this paper, a simple approach based on the modified sol-gel method was conducted and the non-noble cobalt and molybdenum nitride (Co-Mo-N) could be well dispersed on the TiN surface. We extend the research on the TiN based non-noble metal electrocatalysts by reporting the electrochemical behavior of synthesized Co-Mo-N/TiN catalysts and their stability in acid medium.

2. EXPERIMENTAL

2.1. Chemicals

Carbon supported Pt catalyst (40 wt%, Pt/C, Johnson Matthey Fuel Cells), Nafion (5 wt% in a mixture of alcohols and water, DuPont), TiN (20nm, 99.99%, Aladdin Chemical Co., Ltd.), $Co(NO_3)_26H_2O$ (Tianjin Chemical Factory), $(NH_4)_6Mo_7O_{24}4H_2O$ (Tianjin Chemical Factory).

2.2. Synthesis of Co-Mo-N/TiN

$(NH_4)_6Mo_7O_{24}$•$4H_2O$ and $Co(NO_3)_2$•$6H_2O$ were mixed with the solution of citric acid (CA) at a molar ratio of CA:(Mo+Co)=2:1 under continuously magnetic stirring. 25 wt% NH_3•H_2O solution was added drop by drop into the above solution until the pH value of the solution between 2~3. Subsequently, some amounts of nano TiN powder were added into the above solution, corresponding to the mass ratio of cobalt and molybdenum were 4 wt%, 6 wt%, 8 wt%, which were designated as Co-

Mo-N/TiN-4, Co-Mo-N/TiN-6, Co-Mo-N/TiN-8, respectively. Then the mixture was concentrated in a water bath at 80℃ to form the wet gel, finally the gel was dried at 120℃ in air overnight. As-prepared precursors were then calcined and nitrided in NH_3 with a flow rate of 150 mL/min. The nitride temperature was ramped from room temperature to 300℃ by 10℃/min, and then increased from 300℃ to 450℃ at 0.67℃/min, finally held at 700℃ for 2h. When the reaction was completed, products were passivated in 99% Ar/1% O_2 gas at room temperature to prevent the oxidation of Co-Mo-N/TiN samples. The samples of different cobalt and molybdenum molar ratio 1:1, 1:2, 2:1 and pure cobalt or molybdenum were named as Co_1Mo_1Nx/TiN, Co_1Mo_2Nx/TiN, Co_2Mo_1Nx/TiN, Co_2N/TiN and Mo_1N/TiN, respectively.

2.3. Characterization

The crystalline structures of the Co-Mo-N/TiN samples were characterized with a PW3040/60 diffractometer equipped with Cu radiation, operating at 60 kV and 60 mA with the scanning rate of 2 °/min. Scanning electron microscopy (SEM) analysis was done on a JSM 7001F high-resolution microscope. The morphology and microstructure measurements were carried out on a Tecnai G2 F20 field emission transmission electron microscope (HRTEM). X-ray photoelectron spectroscopic (XPS) analysis was performed on the Thermoescalab 250Xi spectrometer, with the monochromatized Al Kα X-rays (1486.6 eV) at 150W. All the binding energies of the Co 2p, Mo 3d of the Co-Mo-N/TiN sample were calibrated with respect to C 1s peak at 284.6 eV.

2.4. Electrochemical Measurements

Electrochemical measurements were conducted with CHI760D Electrochemical Workstation. Catalyst ink for electrochemical testing was prepared by adding 5 mg Co-Mo-N/TiN or 0.75 mg 40 wt% commercial Pt/C catalyst powder and 5 mg carbon black (Vulcan XC72R) into 1 mL mixture of 53.75 vol% double-distilled water, 30 vol% isopropyl alcohol, 20 vol% acetone and 6.25 vol% Nafion (5 wt%, DuPont), sonicated for 30 minutes to disperse the catalyst in the ink. 10 μL of catalyst ink was cast onto a glassy carbon (GC) disk electrode (0.25 cm^2 geometrical areas, Pine Research Instrument) and dried under infrared lamp. The mass of cobalt and molybdenum on the GC disk electrode was about 1.2 mg/cm^2, which was the same as the Pt loading. A conventional three-electrode glass cell was used for all electrochemical measurements at room temperature, with an electrolyte solution of 0.5 M H_2SO_4. Here, the saturated calomel electrode (SCE) was used as the reference electrode, and Pt foil as the counter electrode. Cyclic voltammetry (CV) and rotating disc electrode (RDE) measurements were carried out to evaluate ORR activities. CVs were recorded in 0.5 M H_2SO_4 solutions saturated with O_2 or N_2 gas. All CV and RDE measurements were carried out from -0.2 V to 0.8 V vs. SCE at a scan 10 mV/s rate. And the RDE measurements were collected in O_2 saturated solutions with rotating speed from 0 to 2000 rpm.

3. RESULTS AND DISCUSSION

3.1. Phase Identification and Morphology

The X-ray diffraction (XRD) patterns of Co-Mo-N/TiN samples with different cobalt and molybdenum doping ratio were shown in Fig. 1a. It was illustrated the existence of MoN phase (PDF#25-1367) due to the diffraction peaks at 2θ=31.9°, 36.2°, 49.0°, 74.3°, 78.3°and 85.57° for the different loading ratio Co-Mo-N/TiN catalysts. Co_2N species were verified by the peak at 37.2°, 39.1°,41.6°, 42.8°, 44.4°, 48.5°, 69.5°, 76.8° and 84.5°(PDF#06-0647) . The diffraction peaks of TiN at 36.7°, 42.6°, 61.8°, 74.1° and 78.0° were observed for Co-Mo-N/TiN catalysts. Besides, compared to the diffraction peaks of sample Co_1Mo_1Nx/TiN-4, the intensity of MoN and Co_2N diffraction peaks increased successively in samples Co_1Mo_1Nx/TiN-6 and Co_1Mo_1Nx/TiN-8 due to the increase of MoN and Co_2N content.

The SEM results (Fig. 1b) showed that catalyst surface was filled with irregular small spheres, uniform distribution and the size lies less than 50nm.

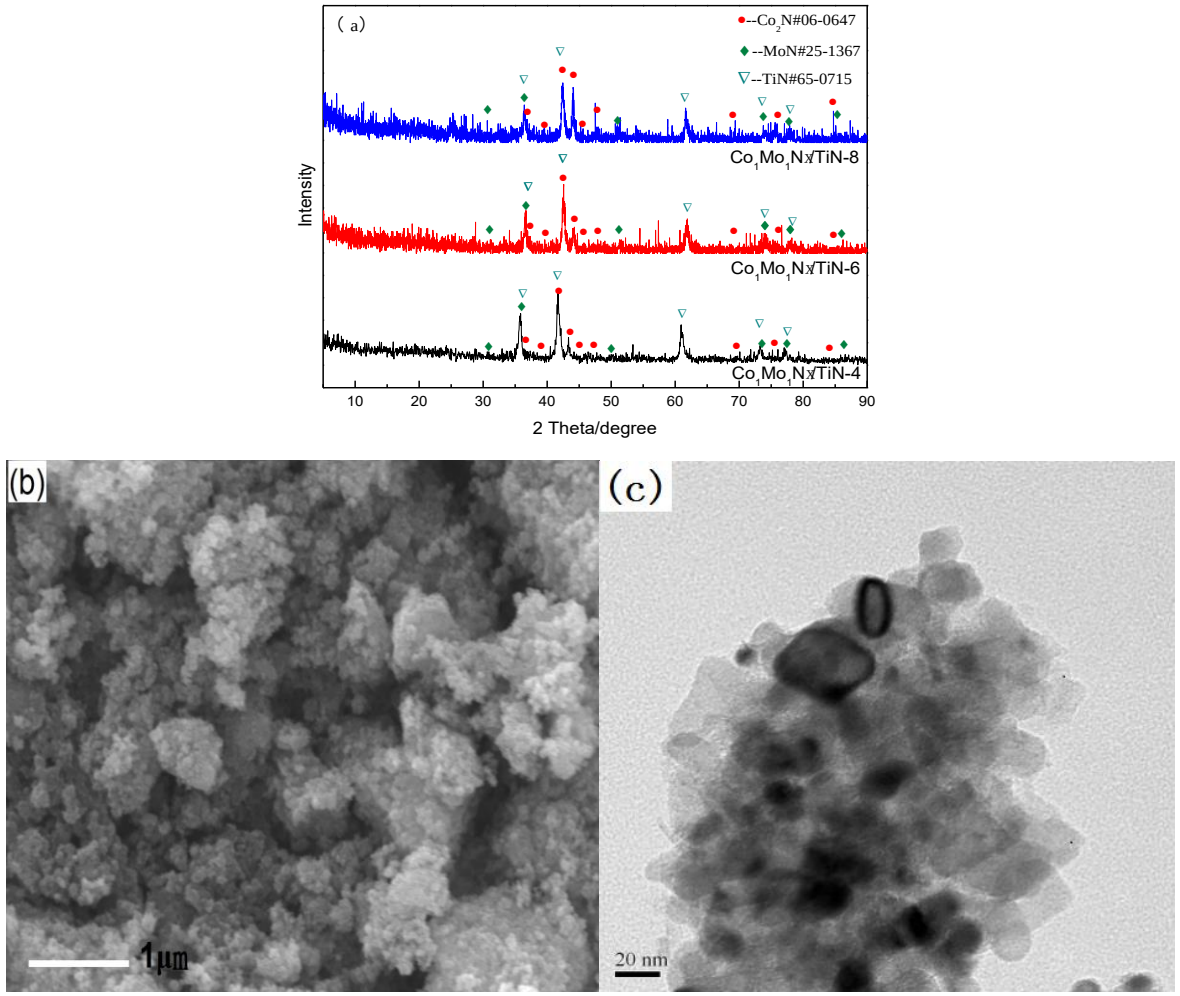

Figure 1. (a) XRD patterns of Co_1Mo_1Nx/TiN-4, Co_1Mo_1Nx/TiN-6 and Co_1Mo_1Nx/TiN-8, (b) SEM image of Co_1Mo_1Nx/TiN-6, scale bar: 1 μm and (c) TEM image of Co_1Mo_1Nx/TiN-6, scale bar: 20 nm.

Three HRTEM images of Co_1Mo_1Nx/TiN-6 were obtained at different regions. Fig. 2a showed the clear lattice fringes with the average distance between the neighboring fringes about 0.212 nm, corresponding to (200) planes of TiN (PDF#65-0715). The successive visible rings in the Fig. 2a were also indicative for a high degree of ordering. Meanwhile, the HRTEM pattern in Fig. 2b imaged MoN planes. The recorded d-value around 0.124 nm ascribed to the MoN (PDF#25-1367) (312) planes. At the same time, in the selected area electron diffraction pattern shown in Fig. 2b, the diffraction halo diameter about 0.124 nm, 0.133 nm, 0.128 nm conformed to MoN (312), (213), (222) planes surface. As shown in fig. 2c, the d-value equals 0.437 nm corresponding to the reflections from the Co_2N (PDF#06-0647) (132) planes. The diffraction halo diameter 0.245 nm, 0.237 nm and 0.230 nm, tallied with Co_2N (PDF#06-0647) (021) (111) (002) planes, respectively. The corresponding electron diffraction presented a smeared halo and the weak but discernible rings implying that the degree of ordering for this portion of the sample was not as high as for a well crystalline one. Additionally, the lattice fringes were in good agreement with the results of XRD. Thus, it is indicated that the nanoscale Co_2N and MoN were successfully loading on TiN by using the modified sol-gel method mentioned.

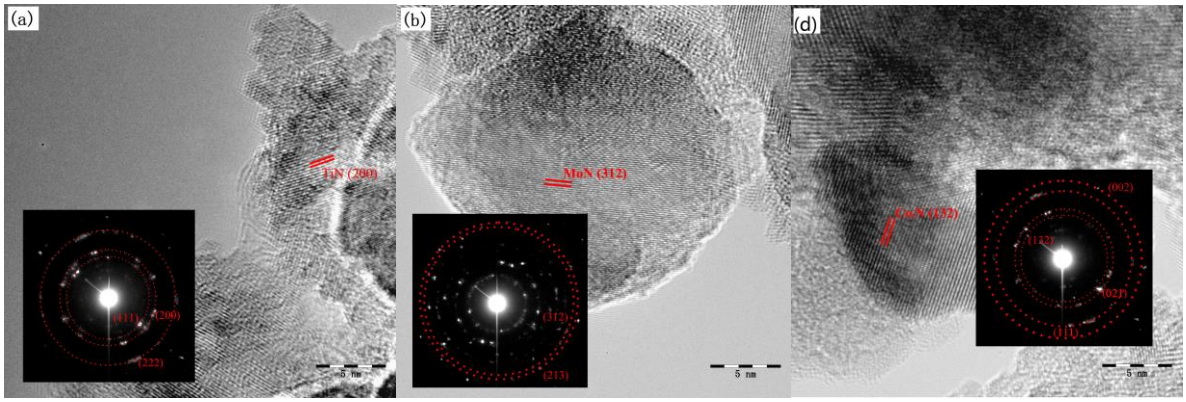

Figure 2. HRTEM images of Co_1Mo_1Nx/TiN-6 at different region, scale bar: 5 nm.

3.2. Spectroscopic analysis of nitride catalyst

To probe the chemical composition and content of nitrogen, cobalt and molybdenum, X-ray photoelectron spectroscopic measurements were prepared. All the binding energies of the Co 2p, Mo 3d of the Co-Mo-N/TiN samples were calibrated with respect to C 1s peak at 284.6 eV. The deconvolution of the Co 2p spectra showed fours peaks (Fig. 3a). The peaks of Co $2p_{3/2}$ and Co $2p_{1/2}$ presented at 781.2 and 797.8 e V, respectively. And the satellite peaks were at around 785.9 and 802.9 eV. This clearly showed the existence of Co^{2+} in the Co-Mo-N/TiN samples [21-23]. And no metallic Co and cobalt oxide was observed in the XRD and XPS results, which indicates Co_2N was successfully synthesized in Co-Mo-N/TiN. The analysis of the Co-Mo-N/TiN Mo 3d XPS spectra were more complex due to a spin−orbit coupling feature. MoO_3 was used as a reference to determine the separation and relative intensities of Mo 3d5/2 and 3d3/2 peaks [24]. Fitting of the Mo 3d XPS data revealed four Mo 3d5/2 species in Fig. 3b. The deconvolution result showed the peaks at 228.7, 229.2, 229.8, and 232.4 eV, which were attributed to Mo^{2+}, $Mo^{\delta+}$ ($2<\delta<4$), Mo^{4+} and Mo^{6+}, respectively. The

surface content of the element was accurately measured by XPS(shown in Table 1). The sum of cobalt and molybdenum on surface was 10.9%, 20.3% and 30%, corresponding to the sample Co_1Mo_1Nx/TiN-4, Co_1Mo_1Nx/TiN-6, Co_1Mo_1Nx/TiN-8, indicating that the non-metallic elements decomposed during heating treatment. Compared with the sample Co_1Mo_1Nx/TiN-4 and Co_1Mo_1Nx/TiN-8 samples, the contents of $Mo^{\delta+}$ in Co_1Mo_1Nx/TiN-6 sample were much higher. The total amount of Mo^{2+} and $Mo^{\delta+}$ species was about 10.21%, 35.07% and 27.03% for the sample Co_1Mo_1Nx/TiN-4, Co_1Mo_1Nx/TiN-6 and Co_1Mo_1Nx/TiN-8, respectively (shown in Table 2). And the Mo^{2+} and $Mo^{\delta+}$ usually exist in the form of MoN. In Fig. 3c, the N1s spectra of the Co-Mo-N/TiN samples were deconvoluted to three peaks at 396.4 eV, 397.2 eV and 399.1 eV. N1s peak around 399.1 eV was associated with N-H groups [25]. The origin of the surface N-H was likely due to an adventitious process such as incompleted reaction with NH_3 or moisture. The major peaks were from Co/Mo−N and TiN, around 396.4 and 397.2 eV, respectively, which confirmed that the surface of Co-Mo-N/TiN remained the nitrides even after air exposure. Along with the increase of the loading ratio, the shape of the N 1s spectra changed, and the ratios of the Co/Mo−N and TiN N 1s peak areas were 0.54, 1.25 and 1.5 for the sample Co_1Mo_1Nx/TiN-4, Co_1Mo_1Nx/TiN-6 and Co_1Mo_1Nx/TiN-8, respectively. The ratio of Co/Mo−N increased which suggested that the Co_2N and MoN species were synthesized on the nano TiN successfully.

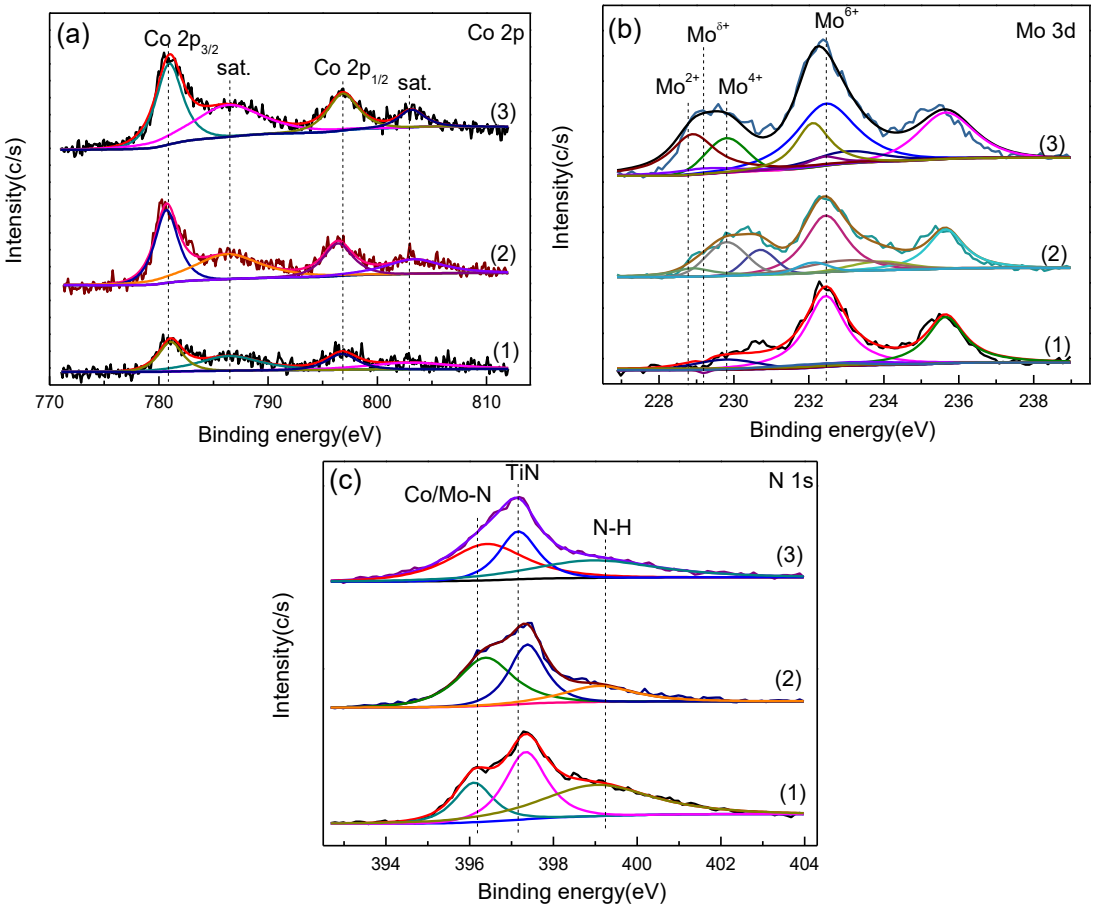

Figure 3. Deconvolution of Co 2p (a), Mo 3d (b) and N 1s(c) of nitride samples: (1) Co_1Mo_1Nx/TiN-4, (2) Co_1Mo_1Nx/TiN-6, (3) Co_1Mo_1Nx/TiN-8.

Table 1. XPS analysis of element contents for different samples

sample	m_{Co}(%)	m_{Mo}(%)	m_{Ti}(%)	m_{C}(%)	m_{N}(%)	m_{O}(%)	$m_{(Co+Mo)}$(%)
Co_1Mo_1N x/TiN-4	5.4	5.5	44	11.5	12.6	21	10.9
Co_1Mo_1N x/TiN-6	11.1	9.2	39.6	7.1	13.2	19.9	20.3
Co_1Mo_1N x/TiN-8	15.4	14.6	35.7	2.8	13.3	18.1	30

Table 2. XPS analysis of molybdenum species for different samples

Sample	Mo^{2+}		$Mo^{\delta+}$		Mo^{4+}		Mo^{6+}	
	B.E. (eV)	Content (%)	B.E. (eV)	Content (%)	B.E. (eV)	Content (%)	B.E. (eV)	Content (%)
Co_1Mo_1Nx/TiN-4	228.7	9.61	229.1	0.60	229.6	13.48	232.4	76.31
Co_1Mo_1Nx/TiN-6	228.7	9.43	229.0	25.64	229.6	14.49	232.3	50.44
Co_1Mo_1Nx/TiN-8	228.7	26.61	229.0	0.42	229.6	22.17	232.5	50.80

3.3. Oxygen reduction reaction activity of nitride catalyst

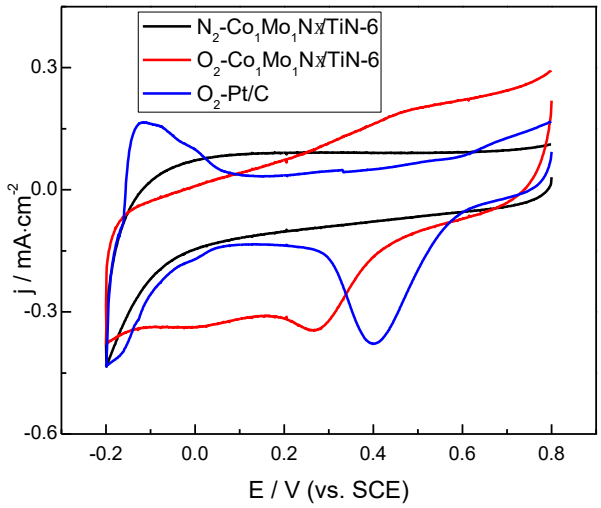

Figure 4. CV curves of catalysts in N_2 or O_2 saturated, 0.5 M H_2SO_4 solution, scan rate 10 mV/s.

ORR catalyst always exhibits poorer activity in acid medium, compared with the one in alkaline medium. TiN supported Pt_1Ag_9 nanoalloy catalysts was synthesized as the ORR catalyst, suggesting that nanoscale TiN is a very promising support in alkaline medium. However, its activity in

acid medium was not investigated [26]. The electro-catalytic properties of the as-synthesized Co-Mo-N/TiN catalysts were examined in N_2 and O_2 saturated, 0.5 M H_2SO_4 electrolyte solutions using cyclic voltammetry (CV) at a scan rate of 10mV/s (shown in Fig. 4). In the case of N_2 saturated solution, the CV curve in the potential range from -0.2 V to 0.8 V (vs. SCE) presented pseudo-capacitive behavior for nitrogen doped mixed-transition metals. In the electrolyte saturated with O_2, Co_1Mo_1Nx/TiN-6 catalyst showed a substantial reduction process with a remarkable reduction peak suited at 0.273 V vs. SCE. Meanwhile, CV curves of the commercial Pt/C($m_{Pt}=m_{(Co+Mo)}$) were also presented in Fig. 4 which reduction peak located at 0.401 V vs. SCE. Compared the reduction peak in O_2-saturated solution, the activity of Co-Mo-N/TiN catalyst was a little lower than Pt/C. To gain additional insight into the ORR process of the as-synthesized catalyst, RDE measurements were further carried out. ORR activity on these catalysts were tested in the O_2-saturated 0.5 M H_2SO_4 solution at a scanning rate of 10 mV/s. Fig. 5a showed the ORR polarization curves of the samples Co_1Mo_1Nx/TiN-4, Co_1Mo_1Nx/TiN-6, Co_1Mo_1Nx/TiN-8 and commercial Pt/C at a rotating rate of 2000 rpm. In order to indentify the impact of cobalt and molybdenum for the ORR activity, the samples Co_2N/TiN-6 and MoN/TiN-6 were synthesized under the same condition as Co_1Mo_2Nx/TiN-6. The ORR onset potential (E_{onset}) for the present work was defined as the potential at which the ORR current was 5% of that measured at -0.2 V, considering that the diffusion-limited current was practically reached at the potential for all catalysts discussed in this work [27]. As expected, it was observed that the onset potential for ORR could reached up to 0.395 V, 0.347 V and 0.189 V (vs. SCE), which were referred to the Co_1Mo_1Nx/TiN-4, Co_1Mo_1Nx/TiN-6 and Co_1Mo_1Nx/TiN-8 catalyst electrode, respectively. $Co_{0.4}Mo_{1.6}N_2$ catalyst synthesized by two step solid-state synthesis procedure showed the similar ORR activity, with an E_{onset} at 0.713V vs. RHE. But there was no comparison with commercial Pt/C and the ORR durability of catalysts in acid medium was not revealed [28]. The onset potential of Co_1Mo_1Nx/TiN-4 and Co_1Mo_1Nx/TiN-6 samples were slightly lower than that of the commercial Pt/C (0.513 V) sample measured under the same condition. Additionally, as shown in Fig. 5a, the current of the sample with Co_1Mo_1Nx/TiN-4 sample was a little larger than the one with Co_1Mo_1Nx/TiN-6, ranging from 0.246 V to 0.395 V, indicating that its ORR performance was somehow a bit better in this current range.

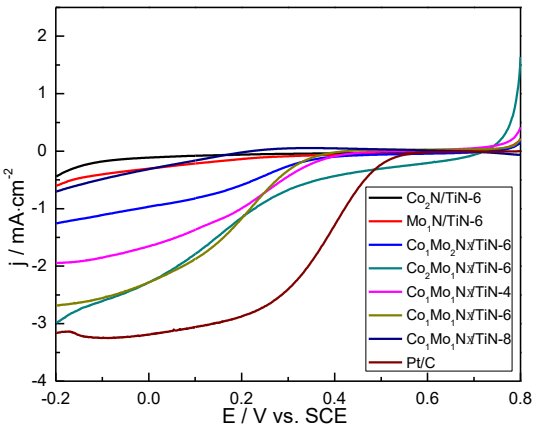

Figure 5. LSV curves of catalysts in O_2 saturated, 0.5 M H_2SO_4 solution with a rotating rate of 2000 rpm, scan rate 10 mV/s.

The different ratio of cobalt and molybdenum had great influence for the ORR current. The current of the samples with different cobalt and molybdenum molar ratio Co_2N/TiN-6, MoN/TiN-6, Co_1Mo_1Nx/TiN-6, Co_1Mo_2Nx/TiN-6 and Co_2Mo_1Nx/TiN-6, ranged from -0.448, -0.616, -2.687, -1.237 to -2.997 mA/cm^2 at the potential -0.2V, denoting that the ORR activity of Co-Mo-N/TiN catalyst were a joint action with cobalt and molybdenum. Analogous conclusion was drawn that cobalt substitution into Mo_2N enhanced the Co-Mo-O-N catalyst activity for acid oxygen reduction reaction [28, 29]. The sample Co_1Mo_1Nx/TiN-6 exhibited the best ORR performance while the total amount of Mo^{2+} and $Mo^{\delta+}$ species in the sample was the highest, compared with the sample Co_1Mo_1Nx/TiN-4 and Co_1Mo_1Nx/TiN-8 (shown in Table 2). Thus we can draw a conclusion that MoN contributed to form the active sites. And it should be noted that the ORR performance of the sample Co_1Mo_1Nx/TiN-6, Co_2Mo_1Nx/TiN-6 were much better at the ORR current, indicating that Co_2N plays an important role in ORR activity sites.

It was reported that robust nanoscale TiN was kinetically stable while MoN was electrochemical unstable in acid medium investigated by cyclic voltammetry for 50 scans in room temperature [30]. Therefore, nanoscale TiN as the catalyst support would enhance the Co-Mo-N/TiN ORR durability. To examine the ORR durability of catalysts in acid medium, a long-term RDE experiment was performed on a glassy carbon (GC) disk electrode in the O_2-saturated 0.5 M H_2SO_4 solution at constant potential of 0.2 V for 5 h (shown in Fig. 6). A constant geometric-based current density was reached after minutes and was almost unchanged during a reaction time of 5 h, denoting a high electrochemical resistance of the catalyst against the applied voltage.

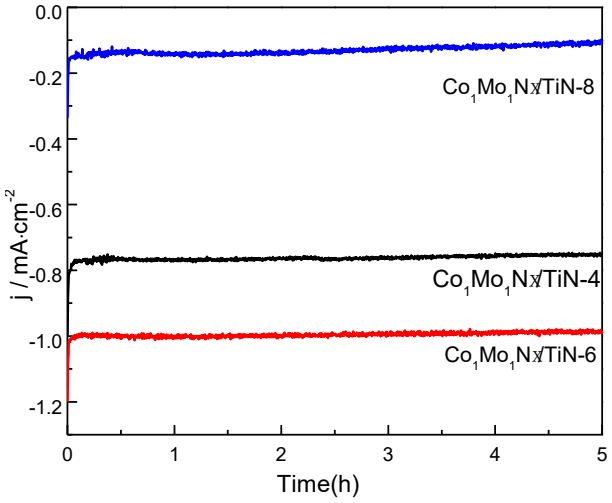

Figure 6. Long-term stability curves of catalysts in O_2 saturated, 0.5 M H_2SO_4 solution with a rotating rate of 1000 rpm, scan rate 10 mV/s.

The RDE polarization curves of oxygen reduction recorded at different rotating speeds (400 to 2000 rpm) were analyzed using the Koutecky-Levich (K-L) equation [31, 32].

$$\frac{1}{j}=\frac{1}{j_k}+\frac{1}{B\omega^{1/2}} \quad (1)$$

Where j represents the measured current density (mA/cm^2), j_k is the kinetically controlled current density (mA/cm^2), ω refers to the angular rotating frequency (rpm), and B is the Levich constant.

$$B=0.62nFC_{O_2}(D_{O_2})^{2/3}\upsilon^{-1/6} \quad (2)$$

Where n denotes the electron transfer number per O_2, F is referred to Faraday constant (96485 C/mol), C_{O_2} is the bulk O_2 concentration (1.7×10^{-2} mol/L), D_{O_2} is the diffusion coefficient of O_2 in the solution (1.3×10^{-5} cm^2/s), v is the kinetic viscosity of electrolyte (1.0×10^{-5} cm^2/s).

Fig. 7 showed the Koutecky-Levich (K-L) plots on the sample Co_1Mo_1Nx/TiN-6. The electron transfer number for the ORR at the sample Co_1Mo_1Nx/TiN-6 were calculated as 4, 3.1 and 1.9 when the different potential was -0.2, 0 and 0.2 V, respectively (shown in Table 3). The ORR on this sample was the mixed electron catalytic process of the two-electron and four-electron pathway throughout the potential range.

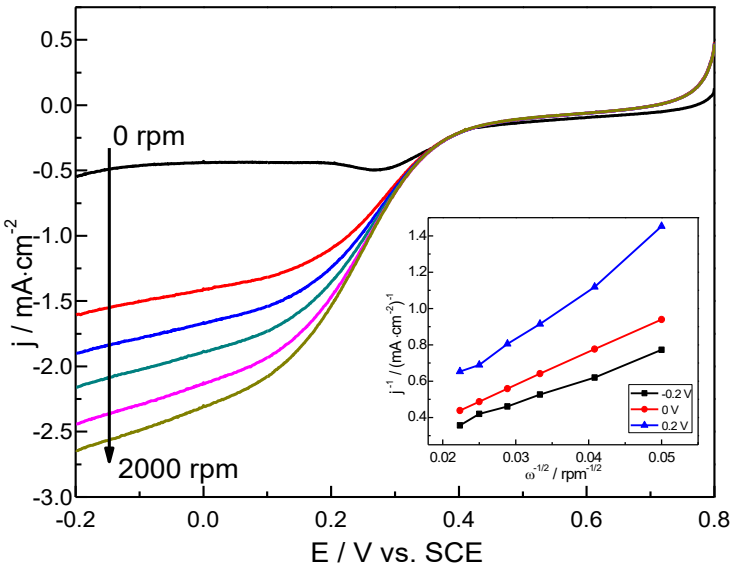

Figure 7. Koutecky-Levich plots for Co_1Mo_1Nx/TiN-6 at various electrode potentials， tested in O_2 saturated, 0.5 M H_2SO_4 solution, scan rate 10 mV/s.

Table 3. Koutecky-Levich plots parameters and number of electrons transferred for ORR on Co_1Mo_1Nx/TiN-6 at different electrode potentials

Potential / V	Slope	Intercept	*n*
-0.2	14	14.05	4.0
0	18.1	0.0343	3.1
0.2	28.93	-0.0271	1.9

4. CONCLUSIONS

In conclusion, the cobalt molybdenum nitrides loading on TiN was synthesized through a simple modified sol-gel method to study the ORR performance of TiN based non-noble metal electrocatalysts. It was found that different contents of cobalt and molybdenum on TiN nanoparticles result in the unequal electrocatalytic property. Further, Co_2N and MoN play important roles in enhancing Co-Mo-N/TiN catalyst activity. The results of long-term stability test showed that Co-Mo-N/TiN has a potential to act as a durable electrocatalyst material. This synthetic is thought to be extended to other TiN based non-noble metal catalysts and thus, might pave the road for the development of active electrocatalysts in acid medium.

ACKNOWLEDGEMENTS
This work was financially supported by National Natural Science Foundation of China(21376056); Yangcheng Scholars Program of Guangzhou, China(1201541563).

References

1. D.W. Wang and D. Su, *Energy Environ. Sci.*, 7 (2014) 576.
2. S. Chen, Z. Wei, X.Q. Qi, L. Dong, Y.G. Guo, L. Wan, Z. Shao and L. Li, *J. Am. Chem. Soc*., 134 (2012) 13252.
3. S. Yang, X. Feng, X. Wang and K. Müllen, *Angew. Chem. Int. Ed.*, 50 (2011) 5339.
4. G. Wu, P. Zelenay, *Acc. Chem. Res.*, 46 (2013) 1878.
5. H. Huang , X. Hu, Zhang, J., N. Su and J. Cheng, *Sci. Rep.*,7 (2017).
6. R. Muntean, D.T. Pascal, G. Mărginean and N. Vaszilcsin, *Int. J. Electrochem. Sci.*, 12 (2017) 4597
7. H.W. Liang, W. Wei, Z.S. Wu, X. Feng and K. Müllen, *J. Am. Chem. Soc.*, 135 (2013) 16002.
8. G. Wu, K.L. More, C.M. Johnston and P. Zelenay, *Sci.*, 332 (2011) 443.
9. L.B. Lv, T.N. Ye, L.H. Gong, K.X. Wang, J. Su, X.H. Li and J.S. Chen, *Chem. Mater.*, 27 (2015) 544.
10. Y. Wang, R. Ohnishi, E. Yoo, P. He, J. Kubota, K. Domen and H. Zhou, *J. Mater. Chem.*, 22 (2012) 15549.
11. F. Jaouen, E. Proietti, M. Lefevre, R. Chenitz, J.P. Dodelet, G. Wu, H.T. Chung, C.M. Johnston and P. Zelenay, *Energy Environ. Sci.*, 4 (2011) 114.
12. Z.Y. Yang, Y.X. Zhang, L. Jing, Y.F. Zhao, Y.M. Yan and K.N. Sun, *J. Mater. Chem.* A, 2 (2014) 2623.
13. R. Kröger, M. Eizenberg, C. Marcadal and L. Chen, *J. Appl. Phys.*, 91 (2002) 5149.
14. V. Lingwal and N.S. Panwar, *J. Appl. Phys.*, 97 (2005) 104902.
15. B. Avasarala and P. Haldar, *Int. J. Hydrogen Energy*, 36 (2011) 3965.
16. H. Kim, M.K. Cho, J.A. Kwon, Y.H. Jeong, E.A. Cho, K.Y. Lee and J.Y. Kim, *Nanoscale*, 7 (2015) 18429.
17. P.P. Patel, M.K. Datta, P.H. Jampani, D. Hong, J.A. Poston, A. Manivannan and P.N. Kumta, *J. Power Sources*, 293 (2015) 437.
18. H. Kim, M.K. Cho, J.A. Kwon, Y.H. Jeong, K.J. Lee, N.Y. Kim, M.J. Kim, S.J. Yoo, J.H. Jang, H.J. Kim, S.W. Nam, S.W. Nam, D.H. Lim, E. Cho, K.Y. Lee and J.Y. Kim, *Nanoscale*, 7 (2015) 18429.
19. B. Avasarala, T.Murray and W. Li, *J. Mater. Chem.*, 19 (2009) 1803.

20. B. Avasarala and P. Haldar, *Electrochim. Acta*, 55 (2010) 9024.
21. D.S. Yang, D. Bhattacharjya, S. Inamdar, J. Park and J.S. Yu, *J. Am. Chem. Soc.*, 134(2012) 16127.
22. A.G. Saputro, H. Kasai, *Phys. Chem. Chem. Phys.*, 17 (2015) 3059.
23. G.Q. Zhang, C.X. Li, J. Liu, L. Zhou, R.H. Liu, X. Han, H. Huang, H.L. Hu, Y. Liu and Z.H. Kang, *J. Mater. Chem.* A, 2 (2014) 8184.
24. B.F. Cao, G.M. Veith, J.C. Neuefeind, R.R. Adzic and P.G. Khalifah, *J. Am. Chem. Soc.*, 135 (2013) 19186.
25. S. Oktay, Z. Kahraman, M. Urgen and K. Kazmanli, *Appl. Sur. Sci.*, 328 (2015) 255.
26. Z. Cui, M. Yang, H. Chen, M. Zhao and F.J. DiSalvo, *ChemSusChem*, 7 (2014) 3356.
27. L. Birry, J. Zagal and J-P. Dodelet, *Electron. Commun.*, 12 (2010) 628.
28. B. Cao, J.C. Neuefeind, R.R. Adzic and P.G. Khalifah, *Inorg. Chem.*, 54 (2015) 2128.
29. B. Cao, G.M. Veith, R.E. Diaz, J. Liu, E.A. Stach, R.R. Adzic and P.G. Khalifah, *Angew. Chem. Int. Ed.*, 52 (2013) 10753.
30. Y. Xiao, Z. Fu, G. Zhan, Z. Pan, C. Xiao, S. Wu and Z. Wei, *J. Power Sources*, 273 (2015) 33.
31. V. Stamenkovic, T.J. Schmidt, N.M. Markovic and P.N. Ross, *J. Phys. Chem.* B, 46 (2002) 11970.
32. E. Salahifar, B. Dadpou and D. Nematollahi, *J. Electroanalytical Chem.*, 782 (2016) 207.